Microstructure, composition and critical currents in melt-textured YBCO ceramics

V.V.Prisedsky, B.A.Tonkin, Y.G.Proykova*, E.M.Roysenblat**, E.I.Volkova, T.J.Oliver*, F.C.Walsh*, J.R.Smith*, N.G.Kisel***

Donetsk State Technical University, Donetsk 340000, Ukraine
* University of Portsmouth, Portsmouth PO1 2DZ, United Kingdom
** Research Institute Reactivelectron, Donetsk 340096,Ukraine

Received January 14, 1996

Grains morphology, texture and grain alignment, variations in chemical composition together with critical currents have been studied as a function of coordinate along the length of elongated melt-textured YBCO rod specimens. Significant inhomogeneities in critical currents and chemical composition (211/123 compositional ratio and oxygen content) were observed for different sections of the specimens. A strong correlation between critical current and compositional parameters has been found.

Изучены морфология, текстура кристаллических зерен, изменения химического состава, а также критические токи в зависимости от координаты вдоль длинномерных стержнеобразных YBCO образцов, полученных расплавной технологией. Для различных участков по длине образцов найдены значительные неоднородности величин критического тока и химического состава. Обнаружена сильная корреляция между критическими токами и композиционными параметрами материала.

Introduction

Critical current densities exceeding 10^4 A/cm^2 at 77 K and 1 T have been achieved in melt processed $YBa_2Cu_3O_{7-y}$ ceramic superconductors [1-2]. The increase in the critical current values is attributed to the reduction of the weak-link effects as a result of grain growth and grain alignment in the melt-texturing process. In such specimens, an excess of Y_2BaCuO_5 (211) phase is always formed in originally pure $YBa_2Cu_3O_{7-y}$ (123) material due to incomplete peritectic reaction. These 211 phase inclusions are considered to be possible centres for magnetic flux pinning [3]. The 211 phase may also affect the critical current density indirectly giving rise to an enhanced density of pinning centres such as dislocations, stacking faults and other extended defects [4].

It is important to assess the role of possible technological inhomogeneities in the melt-texturing process. For this purpose, we report here investigations of the microstructure and chemical composition together with critical current density distribution along the length of bar specimens of melt-textured $YBa_2Cu_3O_{7-y}$ ceramics.

Experimental

Chemically pure Y_2O_3, $Ba(NO_3)_2$ and CuO or CuO_2 were used as the main starting materials. To improve electrophysical properties, minor additives of Mn, Zr and W oxides were substituted for some part of copper oxide so that the composition of initial superconducting material corresponded to the formula $YBa_2Cu_{2.96}Mn_{0.02}Zr_{0.01}W_{0.01}O_{7-y}$ [5]. This starting material was synthesised by conventional solid-state reaction with a maximum temperature of 800°C for 3 hours. Then, elongated rectangular bars with typical dimensions of 100×2×2 mm were pressed and sintered at 920°C for 20 h and at 970°C for 20 h and then cooled to 450°C at 100°C/h.

A variation of zone-melting technology [5] was used for production of textured samples. The sintered specimens underwent heat treatment in

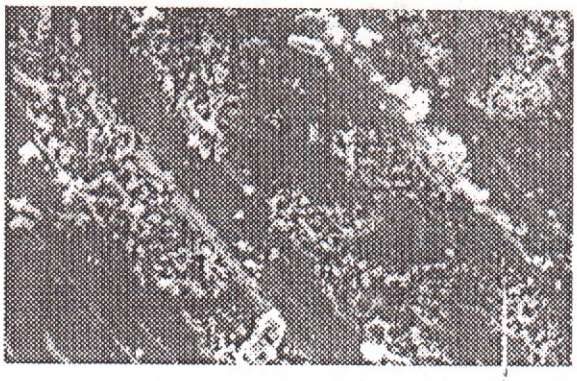

a

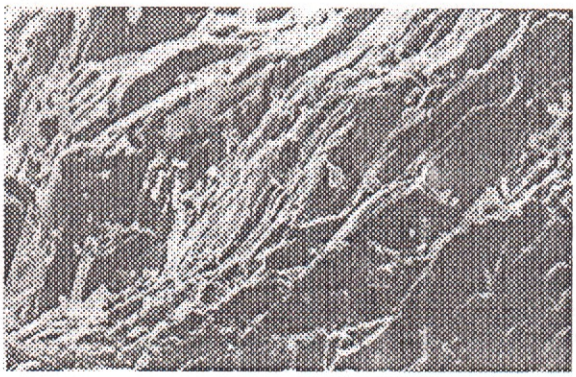

b

Fig.1. Scanning electron microphotographs taken from the upper surface of the melt-textured rod specimen (a) and from one of its cleavage surfaces (b).

air ambient in a horizontal tube furnace of a special design in which the temperature profile had a gradient of not less than 50°C/cm at the end of the heating zone. The specimens were placed on alumina substrates covered with powdered mixture of $BaTiO_3$ and Y_2O_3 (2:1 by weight). The maximum temperature in the heating zone was chosen individually for each batch with precision of ±1°C in the 1110–1120°C interval. The velocity of sample transport through the heating zone was 2 mm/h.

After that, the bar specimens were oxidized in oxygen atmosphere at 600°C for 1 h, cooled to 570°C at 6°C/h and then to 450°C at 60°C/h. Following 5 h at this temperature the specimens were cooled to 400°C where they remained for a further 5 h, before furnace cooling to room temperature in a continuous oxygen flow. Prior to treatment in oxygen atmosphere, silver paste electrodes spaced 7–10 mm apart along the length of the specimen were employed onto the specimens.

The grain composition and microstructure were studied by analytical scanning electron microscopy (SEM) using a JEOL JSM-35C instrument equipped with an energy dispersive X-ray spectrometric (EDS) electron probe (EPMA). A Phillips PW 1710 based diffractometer was used for X-ray diffraction measurements using Co K_α radiation. Fragments broken from long bars as well as crushed powdered samples prepared from them were studied. A Debye-Scherrer camera operated in rotation mode was applied to study the character and degree of texturing in the samples. Atomic force microscopy (AFM) studies were performed in air under ambient conditions using a Discoverer Topometrix TMX2000 Scanning Probe Microscope (SPM). A 70 μm scanner was used and imaging was performed at a scan rate of 120 $\mu m \cdot s^{-1}$ in contact mode using forces in the range of 1 to 50 nN. Standard profile silicon nitride tips were used for contact mode imaging. Graphical output was displayed on a monitor with a resolution of 400 lines×400 pixels. Images were levelled by plane-fitting and left-shading was used to enhance topographic features.

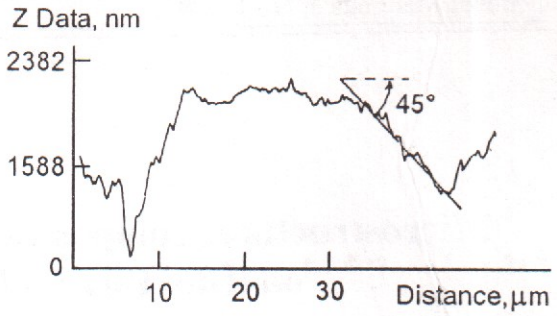

Fig.2. The AFM height profile across one of the large grains on the upper surface of the specimen.

Transport critical currents in various sections of elongated bar specimens were measured by four-probe impulse method at 77 K [6]. For estimation of critical current, I_c, the criterium $E < 1$ μV was used.

Results and discussions

As seen in the SEM micrographs taken from different faces of the elongated superconducting bars, the stacks of large plate-like grains are typical for the microstructure of melt-processed specimens (Fig.1). These large grains lie at approximately 45° to the bars longest axis and are separated on the outer faces of the bars by smaller grains. These smaller grains are often seen also on the cleavage surfaces of the samples. An AFM height profile (Fig.2) provides more quantitative characteristic for one of the large plate-like grains seen in the surface of a bar sample. The grain, lying at 45° to horizontal (i.e. bar facial) plane, is ~ 27 μm thick as calculated from the data shown in Fig.2.

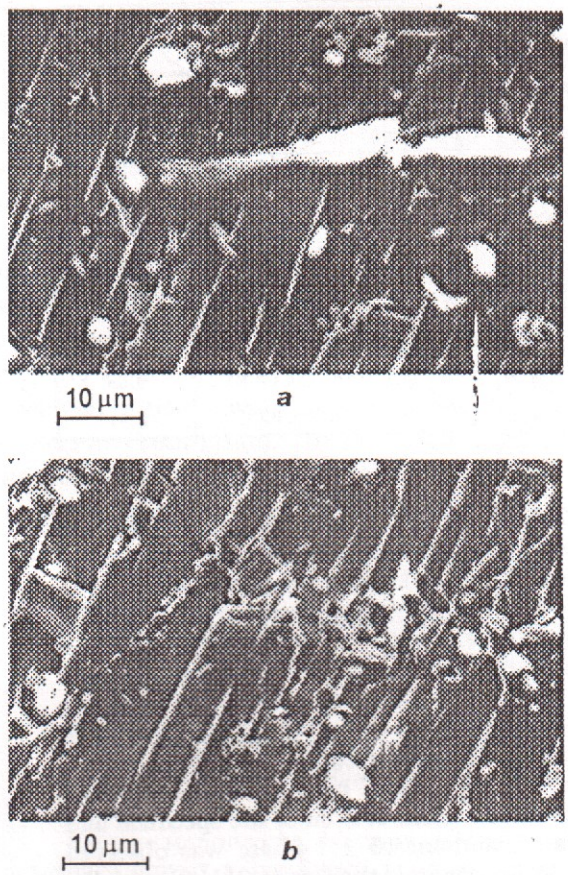

Fig.3. Typical SEM images showing grain alignments in cross-section cut perpendicular to the specimen largest axis.

The character of the large grain alignment is more readily seen in micrographs taken from cross-sections cut perpendicular to the bar axis (Fig.3). Large plate-like grains 10–30 μm thick extend very often through the whole geometrical volume of the bar. The regular alignment of these plate-like grains is sometimes interrupted either by large plate-like grains of another crystallographically equivalent orientation (Fig.3a) or by smaller randomly oriented grains which are often rather circular in cross-sections (Fig.3a,b). Results of electron microprobe analysis (Fig.4) show that the chemical composition of large plate-like grains corresponds in most cases to $YBa_2Cu_3O_{7-y}$ (123 phase). In a few cases, we observed plate-like grains of Y_2BaCuO_5 (211 phase) but, more often, the composition analysis identified intergrowths of 123 and 211 phases with the average compositional ratio close to 1:1. The composition of the smaller grains was usually found to be Y_2BaCuO_5, but sometimes $YBa_2Cu_3O_{7-y}$ needle-shape small grains were also found during the analysis. However, small grains with intermediate composition, as in intergrowths, were never observed.

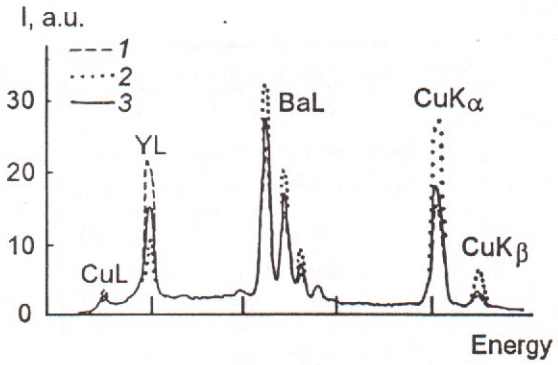

Fig.4. Energy dispersive spectra taken by locating the electron probe on various grains and showing three observed compositions for plate-like grains: 211 phase (1); 123 phase (2); an intergrowth of 123 and 211 phases (3).

The diffraction patterns taken in the PW 1710 based diffractometer from the whole bar specimens oriented with their longest axis perpendicular to the incident X-ray beam showed all the peaks belonging to 211 phase but practically no reflections from grains of 123 phase. Comparing this fact with SEM data on grain morphology and composition, we conclude that smaller 211 grains in the specimen are randomly oriented and produce a diffraction pattern of powder type. At the same time, 123 phase is strongly textured and its grains give no diffraction peaks under the applied geometry of X-raying.

To study the character and degree of the texture in large grains, the fragments cut from the bar specimens have been X-rayed in the Debye-Scherrer camera operated in rotation mode using several different orientations of the bar longest axis with respect to the rotation axis. In the photos with recorded diffraction patterns, continuous diffraction rings from 211 grains are fixed. Reflections from 123 grains are seen as groups of narrow-spaced spots. A strong alignment of all three orthogonal crystallographic axes in different grains is evident from these data. The studied melt-textured specimens represent a «block structure» close to a single crystal. The possible misorientation of crystallographic axes between various large 123 grains is assessed to be a few angle degrees. But the most essential type of grain misorientation is the observed change of *c* axis orientation by 90°, i.e. the change of the orthorombic distortion in different grains between {100} equivalent directions of the cubic perovskite structure. This type of crystallographic misorientation may be related to the observed by SEM large-angle misorientations of plate-like grains (Fig.3a).

Measurements of critical currents I_c in different sections along the length of melt-textured bar

Table 1.

Parameter	Section along the length of the bar					
	a	b	c	d	e	f
Specimen 138						
I_{211}/I_{123}	0.159	0.141	0.060	0.032	0.050	0.084
$x(0)$	6.83	6.80	6.88	6.85	6.92	6.84
$I_c(0)$	90	90	>130	110	>200	130
$I_c(0.3)$	70	90	>200	>160	2[illegible]0	30
Specimen 147						
I_{211}/I_{123}	0.274	0.123	0.102	0.229	0.077	
$x(0)$	6.80	6.85	6.88	6.85	6.90	
$I_c(0)$	80	160	>140	>150	>200	
$I_c(0.3)$	20	200	200	140	20	

specimens showed considerable variations in I_c values. To approach the nature of these inhomogeneities in melt-texturing process, these sections (excluding the material under the electrodes) were cut from the rods after electrical measurements, then crushed and ground in an agate mortar into a fine powder and X-rayed in the diffractometer. Considerable variations in relative amounts of 123 and 211 phases as well as in 123 unit cell parameters were noticed (Table 1).

The relative amounts of 211 and 123 phases were assessed from X-ray diffraction data (Fig.5 and 6) as the ratio of intensities I_{211}/I_{123} of strongest peaks for these two phases. The oxygen content, given in the Table 1 as oxygen formula index x(O), was also determined for the same sections of the samples. For that purpose, d_{006}, d_{200}, d_{020} spacings were determined from diffraction patterns. The calibration dependence of

Table 2.

Parameters		Linear regression equation	Correlation coefficient
x	y		
Specimen 138			
I_{211}/I_{123}	$x(0)$	$y = -0.814x+6.93$	0.85
I_{211}/I_{123}	$I_c(0)$	$y = -790x+206$	0.85
I_{211}/I_{123}	$I_c(0.3)$	$y = -1210x+242$	0.87
Specimen 147			
I_{211}/I_{123}	$x(0)$	$y = -0.396x+6.92$	0.89
I_{211}/I_{123}	$I_c(0)$	$y = -605x+255$	0.91

006/200/020 d-space values on oxygen content was found in preliminary X-ray measurements of 123 samples with known oxygen content. The values of transport critical currents across the complete cross-section of the bars measured in zero magnetic field, $I_c(0)$, and in magnetic field 0.3 T, $I(0.3)$, are given in Table 1. In both the specimens studied, a drop in I_c (0.3 T) value is observed for terminal sections of the bars.

A strong correlation between the critical current values in a given section of the specimen and the relative amount of 211 phase was observed (Table 2). In general, the less is 211 content the higher is critical current. We may conclude that, for studied interval of experimental conditions, the obtained amount of 211 phase is excessive. Evidently, 211 phase should not be present as large grains that are observed in the studied samples. From the other side, the correlation between the amount of 211 phase and oxidation state of 123 phase was also found, as seen from Table 2. The increase in 211 content hinders the effective oxidation of melt-processed YBCO material.

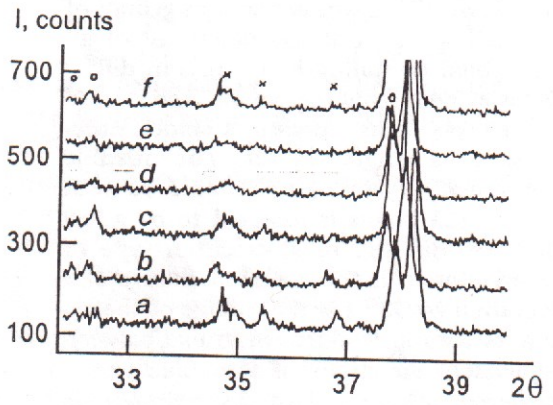

Fig.5. Fragments of X-ray powder diffraction patterns obtained from various sections (*a-f*) along the length of specimen 138. The peaks relating to 123 phase are marked with circles (0) and those relating to 211 phase with crosses (x).

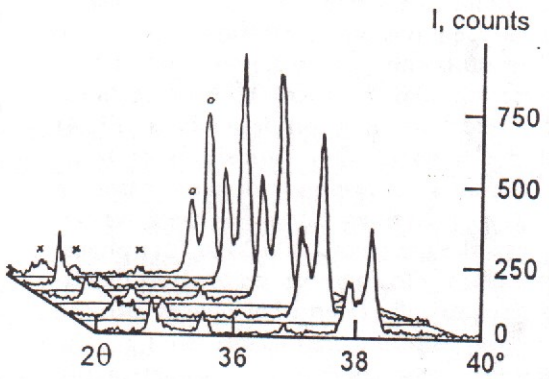

Fig.6. Fragments of X-ray powder diffraction patterns obtained from various sections (*a-e*) along the length of specimen 147. The peaks relating to 123 phase are marked with circles (0) and those relating to 211 phase with crosses (x).

Conclusions

Grain morphology, texture and grain alignment, variations in chemical composition together with critical currents have been studied as a function of co-ordinate along the length of elongated melt-textured YBCO rod specimens. Significant variations in critical currents and chemical composition (211/123 compositional ratio and oxygen content) were observed for different parts of the specimens. A strong correlation between critical current and compositional parameters has been found. The results obtained in this study help to improve the technology of melt-processed superconducting ceramics.

References

1. S.Jin, T.H.Tiefel, R.C.Sherwood et al., *Appl.Phys. Lett.*,**52**, 2074 (1988).
2. M.Murakami, M.Morita, K.Doi, K.Miamoto, H.Hamada, *Jpn.Appl.Phys.*, **28**, L332 (1989).
3. D.F.Lee, V.Selvamanickam, K.Salama, *Physica C*, **202**, 83 (1992).
4. D.Muller, M.Ullrich, K.Heinemann, and H.C.Freyhardt, *Appl.Superconductivity*, 329, (1993).
5. E.M.Roysenblat, S.I.Yermolina, N.G.Kisel et al., Materialovedeniye vysokotemperaturnych sverkhprovodnikov (Abstracts), Kharkov, (1995), p.139 [in Russian].
6. V.V.Klimov, E.M.Roysenblat, S.I.Yermolina, *Superconductivity: Physics, Chemistry, Technology*, **5**, 757 (1992).

Мікроструктура, склад та критичні струми в розплавно-текстурованій кераміці YBCO

В.В.Приседський, Б.А.Тонкін, Й.Г.Пройкова, Е.М.Ройзенблат, Е.І.Волкова, Т.Дж.Олівер, Ф.К.Уолш, Дж.Р.Сміт, Н.Г.Кисель

Вивчено морфологію, текстуру кристалічних зерен, зміни хімічного складу та значень критичного струму в залежності від координати вздовж довгомірних стержнеподібних YBCO зразків, одержаних розплавною технологією. Для різних ділянок по довжині зразків знайдено значну неоднорідність величин критичного струму і хімічного складу. Виявлено сильну кореляцію між критичними струмами та композиційними параметрами матеріалу.